Journal of Cleaner Production 259 (2020) 120923

Contents lists available at ScienceDirect

Journal of Cleaner Production

journal homepage: www.elsevier.com/locate/jclepro

Study of the basic mechanical properties and degradation mechanism of recycled concrete with tailings before and after carbonation

Tao Li [a, b, *], Sheliang Wang [a], Fan Xu [a], Xiangyin Meng [c], Binbin Li [d], Meng Zhan [e]

[a] School of Civil Engineering, Xi'an University of Architecture and Technology, Xi'an, 710055, China
[b] College of Urban, Rural Planning and Architectural Engineering, Shangluo University, Shangluo, 726000, China
[c] Key Laboratory of Concrete Structure Safety and Durability in Shaanxi Province, Xijing University, Xi'an, 710123, China
[d] Key Laboratory of Structure Engineering and Earthquake Resistance, Ministry of Education(XAUAT), Xi'an University of Architecture and Technology, Xi'an, 710055, China
[e] College of Architecture Engineering, Huanghuai University, Zhumadian, 463000, China

ARTICLE INFO

Article history:
Received 14 September 2019
Received in revised form
14 February 2020
Accepted 3 March 2020
Available online 5 March 2020

Handling Editor: Baoshan Huang

Keywords:
Recycled concrete with tailing
Mechanical properties
Microscopic characteristics
Deterioration mechanism

ABSTRACT

Based on the fine powder and the activation characteristics of iron tailings, the basic mechanical properties and deterioration mechanism of the recycled concrete with tailings before and after carbonization were macroscopically and microscopically analyzed via rapid carbonization tests. The macroscopic results showed that the cubic compressive strength increased first and then decreased with the tailings addition at different dosages, with a peak value of 30%. The values of the splitting tensile strength and axial compressive strength fluctuated differently, and the tailings content ranged from 20% to 40% at the peak point before and after carbonization. The peak strain and elastic modulus of recycled concrete were reduced to different extents, and the longer the carbonization age was, the greater the reduction range was. Simultaneously, the carbonization age also increased the brittleness of recycled concrete, causing the descending section of the constitutive curve to greatly fluctuate. Microscopically, the influence of tailings on the matrix structure of the recycled concrete was verified by energy dispersive spectrometer (EDS) and scanning electron microscope (SEM) analysis. The results proved that the appropriate tailings content could improve the interface transition zone (ITZ) and the compactness of the concrete, also optimize the mechanical properties of the recycled concrete. However, excessive tailings could reduce the integrity of the matrix structure, increase the number of harmful pores. According to the research, when the tailings content was 20%–40%, the recycled concrete had high mechanical properties and reasonable microstructure. This study provided a theoretical basis for the popularization and application of the recycled concrete with tailings.

1. Introduction

Tailings and construction waste are inevitable products of accelerated urbanization construction and rapid economic development. Due to the immaturity of regeneration technology, a large number of tailings ponds and construction waste treatment plants exist, which not only occupy land, waste resources, and pollute the environment but also pose a substantial threat to the property and personal safety of the surrounding residents (Li al., 2018; Kox et al., 2019; Lu et al., 2018). Currently, making recycled concrete from tailings and construction waste is the most effective approach.

However, at present, most studies worldwide have been focused on concrete with tailings or recycled aggregate concrete (RAC). In these investigations, the effects of aggregates, such as tailings, and natural coarse aggregates (NCA) on dam concrete were compared, their mechanical properties and frost resistance were discussed. The studies demonstrated the feasibility of using tailings as the aggregate to completely replace an ordinary aggregate in dam concrete (Lv et al., 2019). Cheng et al. (2016) studied the mechanical and chemical activation of iron tailings and the performance of concrete after the partial replacement of cement. The results showed that the compressive strength of concrete decreased gradually with the replacement rate. Shettima et al. (2016) used iron tailings to replace river sand in concrete, and studied its

* Corresponding author. School of Civil Engineering, Xi'an University of Architecture and Technology, Xi'an, 710055, China.
E-mail address: litao623114@126.com (T. Li).

https://doi.org/10.1016/j.jclepro.2020.120923
0959-6526/

Acronyms list

EDS	Energy Dispersive Spectrometer
SEM	Scanning Electron Microscope
IOT-RAC	iron ore tailings in recycled aggregate concrete
NCA	natural coarse aggregate
RCA	recycled coarse aggregate
IOT	iron ore tailings
RAC-*i*	*i*th iron ore tailings in recycled aggregate concrete
NAC	natural aggregate concrete
RAC	recycled aggregate concrete
ITZ	interface transition zone

compressive strength, splitting tensile strength, elastic modulus and durability, the results showed that the strength and elastic modulus of the modified concrete were higher than that of ordinary concrete due to the addition of tailings. Qi et al. (2018) researched a cemented backfill with abandoned tailings and established a corresponding reliable strength prediction model with different intelligent algorithms, which greatly reduced the number of mechanical tests required. Tiwari et al. (2016) summarized various industrial byproducts (such as bottom ash, foundry waste sand, copper slag and tailings) as potential aggregate substitutes in their concrete manufacturing process and summarized the corresponding feasibility, strength and durability. Tang et al. (2019) studied the workability, mechanical properties and durability of concrete with iron tailings. When the iron tailing content was 25%–50%, the mechanical properties improved. Zhang et al. (2013a,b) prepared tailing concrete by replacing river sand with iron tailing powder. The results indicated that when the content of iron tailing powder was 23%, the strength of concrete developed faster. Through the research, it could be seen that the tailings had the characteristics of fine powder and volcanic ash activation (Dandautiya and Singh, 2019). Therefore, the blending of tailings into concrete could help promote the hydration of cementitious materials and improve the strength and durability of concrete (Thomas et al., 2019).

Alternatively, recycled concrete has also been extensively studied along with the accumulation of construction waste. Compared with the natural coarse aggregate (NAC), the RAC has become more complicated due to the large number of new and old interface transition zones (ITZs). The results of scholars worldwide have shown that the mechanical properties of the RAC were reduced to varying degrees (Ferreira et al., 2011; Sani et al., 2005; Zhang et al., 2011). Therefore, research on the performance improvement of the RAC has become a hot topic at this stage. Lu et al. (2019) carbonized the RCA, and then studied the properties and microstructure of the recycled concrete. Microscopic studies showed that carbonization reduces the pore size of the matrix and can effectively improve the hardness of the ITZs. Albayati et al. (2018) treated the coarse aggregate of recycled concrete with lime, tested the modulus and tensile strength of asphalt concrete made from a recycled aggregate and a low-temperature asphalt mixture. Shaban et al. (2019) treated the RCAs with different dosages and different soaking times of a pozzolanic cement slurry, and the surface micro-properties of the recycled aggregates were studied by scanning electron microscopy (SEM) and energy dispersive spectrometry (EDS). The results showed that this kind of soaking method could mitigate the defects that caused poor mortar adhesion and improve the performance of the RCA. The above methods could improve the performance and strength of recycled concrete, but at the cost of a complicated operation, which is not conducive to a wide range of engineering applications.

The use of tailings to enhance the properties of recycled concrete seems to be a good choice. However, research studies on iron ore tailings in recycled aggregate concrete (IOT-RAC) by relevant scholars has lagged behind, and the literature is scarce. Vijayaraghavana et al. (2017) set up 28 concrete mix proportion with different amounts of copper slag, iron slag and recycled aggregate in fine and coarse aggregates. Studies had shown that when 40% copper slag, 40% iron slag and 25% recycled aggregate were added, the recycled aggregate had higher strength than the conventional concrete. Wei et al. (2019) conducted an experimental study on the mechanical properties of the IOT-RAC. The mechanical properties of recycled concrete first increased and then decreased with increasing tailings content. Cui et al. (2018) developed a preliminary design for the mix proportion and studied the cubic compressive performance of the IOT-RAC; the results showed that the compressive strength of the concrete met the requirements of the code when the mix proportion was selected properly.

To compensate for the weak research foundation of the IOT-RAC, in this paper, its mechanical properties and deterioration mechanism are systematically analyzed and studied from macroscopic and microscopic levels to determine the optimum amount of iron tailings and lay a theoretical foundation for engineering applications.

2. Material properties

2.1. Conventional materials

Qinling Portland cement (PO 42.5) was used in this test. The NCA with a size of 5–20 mm was artificial gravel with continuous gradation, and the fine aggregate was sourced from the Bahe River. The particle gradation diagram is presented in Fig. 1(a). For detailed microscopic analysis, the main elements were determined by EDS, as shown in Fig. 2 and Table 1, Table 2, Table 3.

2.2. Recycled coarse aggregate (RCA)

The RCA, produced by an environmental protection company in Xi'an, was a typical material in the current market, in which the brick content was approximately 30%. The selected aggregate had been in service for 30 years and was continuously graded, procedures such as screening, washing, drying, and bagging were used for testing. The main performance and particle gradation are shown in Table 3 and Fig. 1(b).

2.3. Iron ore tailings (IOT)

The experimental iron tailings came from the Yaogou tailings pond, Shaanxi Province. Its main mechanical properties and the particle size distribution are shown in Table 3 and Fig. 1 (c).

3. Experimental methods

The main tests were carried out in the Key Laboratory of Concrete Structure Safety and Durability in Shaanxi Province, while the EDS analyses were conducted at the Materials Analysis and Testing Center of Chang'an University.

3.1. Experiment projects

In this paper, the basic mechanical properties, including the cubic compressive strength, splitting tensile strength, axial compressive strength, deformation property and stress-strain constitutive curve, were taken as basic performance indexes to

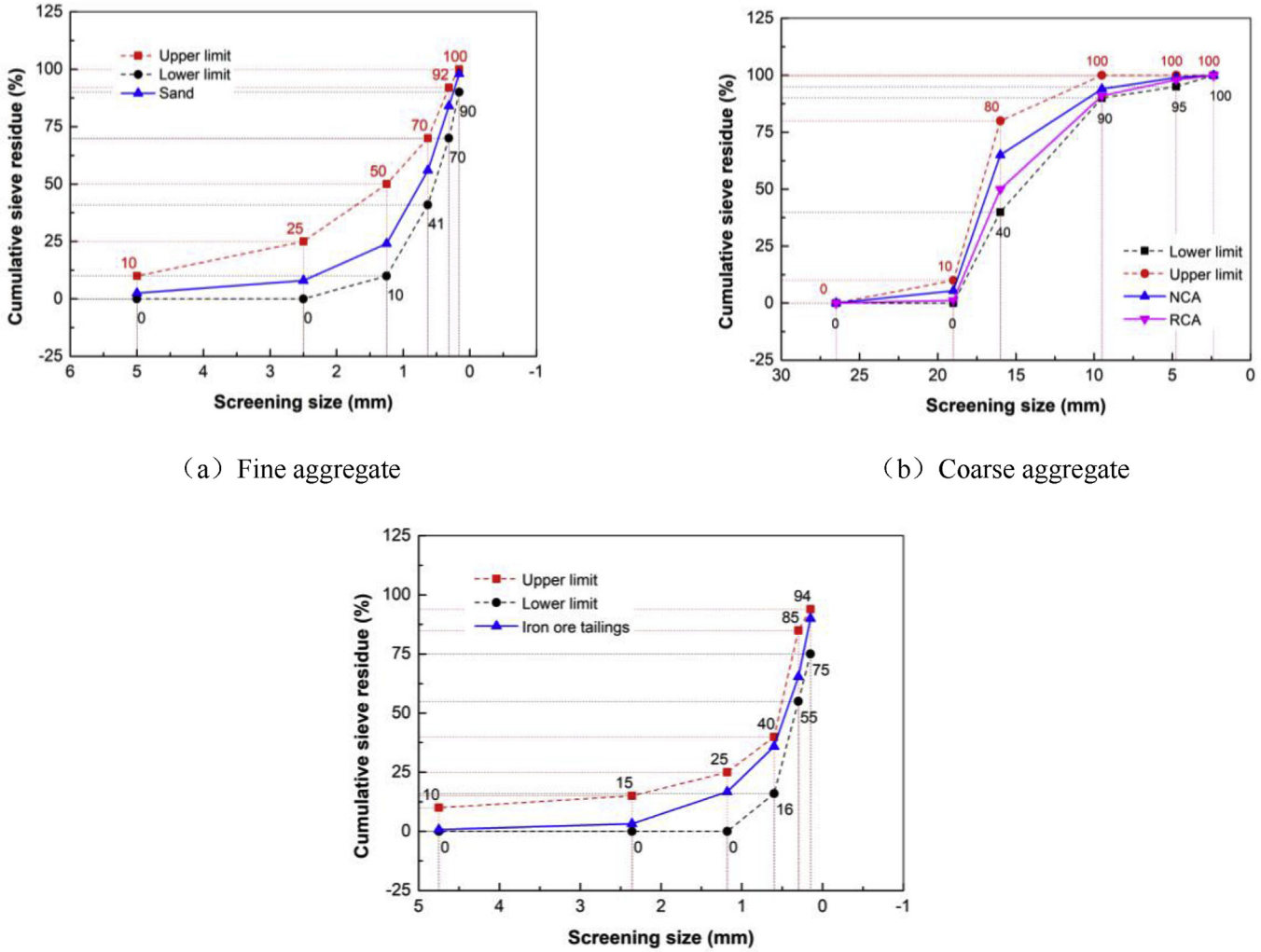

Fig. 1. Particle gradation diagram of the aggregate.

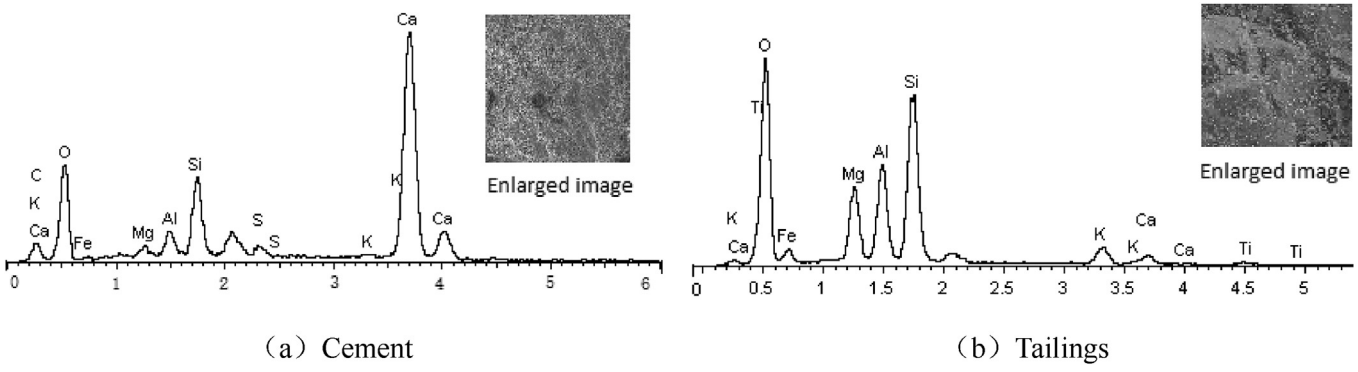

Fig. 2. Energy spectrum analysis of the cement and tailings.

Table 1
Mineral composition of the cement and tailings.

Mineral Composition	C	O	Mg	Al	Si	S	K	Ca	Fe	Ti
Cement(%)	4.12	47.54	0.74	1.54	6.11	1.10	0.53	56.85	0.93	–
Tailings(%)	0	56.49	6.95	8.38	17.46	–	3.02	1.68	5.28	0.74

Table 2
Main performance indicators of the cement.

Water requirement for normal consistency/%	Initial setting time/min	Final setting time/min	Fineness modulus (45 μm)	Stability	Flexural strength (MPa)		Compressive strength (MPa)	
					3d	28d	3d	28d
28	160	280	2.8	Qualified	5.2	6.8	19.5	42.2

establish the strength model of the IOT-RAC, and the corresponding test block sizes were 100 mm × 100 mm × 100 mm, 100 mm × 100 mm × 300 mm, 100 mm × 100 mm × 100 mm, 100 mm × 100 mm × 300 mm, 100 mm × 100 mm × 300 mm. In the test, the recycled concrete blocks of different tailings dosages before and after carbonization were tested. The un-carbonized ages were 7 d, 14 d, 28 d and 90 d.

3.2. Experimental instruments

Through the replacement of the fixture, the main mechanical properties of the test were determined by a 1000 kN microcomputer-controlled electrohydraulic servo universal testing machine, while the stress-strain curve were measured synchronously by the electrohydraulic servo universal testing machine and the MTI-3D noncontact strain measuring system. A TH-W concrete carbonization test box was used for the carbonization, and the loading and carbonization tests were carried out in accordance with the specifications (Ministry of Housing and Urban-Rural Construction of the People's Republic of China, 2009, 2015). Moreover, the specific process of the carbonization test is shown in Fig. 3.

3.3. Experimental conditions and mix proportion design

To save resources and reduce the test amount, the replacement amount of recycled aggregate was selected as 30% (Xiao et al., 2018; Yang et al., 2017; Wang et al., 2013), and then the different proportions of iron tailings were considered. According to the "Technical Standard for Recycled Concrete Structures"(Ministry of Housing and Urban-Rural Construction of the People's Republic of China, JGJ/T 443-2018), the mix ratio was designed with reference to relevant codes and references(Ministry of Housing and Urban-Rural Construction of the People's Republic of China, JGJ55-2011; Gu, 2019; Wang and Dong, 2018). To facilitate the comparative analysis, the water-to-binder ratio was 0.4, the sand ratio was 0.35, and the concrete was subjected to the second mixing method. After trial mixing and adjustment, the mix design of concrete under various working conditions are shown in Table 4.

4. Experimental results

4.1. Cube compressive strength

Fig. 4 shows the variation curve of the cubic compressive strength of the RAC with the tailings substitution rate at different ages before and after carbonization.

In the figure above, it can be seen that different tailings incorporation ratios had different effects on the compressive strength of the concrete cubes. When the dosage was less than 30%, the compressive strength increased with increasing tailings content, while above 30%, the opposite trend occurred, which was consistent with the results of some studies (Shettima et al., 2016; Goyal et al., 2015; Zhang et al., 2013a,b). However, the results showed that the optimum amount of tailings was 25% (Shettima et al., 2016) and 20%–40% (Zhang et al., 2013a,b) respectively.

When the tailings substitution rate was 30%, the compressive strength reached a peak, and the intensity value was close to the corresponding intensity value of the NAC. Simultaneously, the dotted line in Fig. 4 exhibited the corresponding cubic compressive strength values of the NAC and RAC-1 at each age. From Fig. 4(a), when the curing age was small (7 d), the strength values of the RAC tended to increase with different proportions of tailings, but it was smaller than that of NAC. However, when the curing age continued to increase, the concrete strength values

Table 3
Performance indicators of the major aggregates.

Performance criteria	Apparent density kg/m^3	Bulk density kg/m^3	Fragmentation index/%	Water absorption/%	Mud content/%	Water content/%	Organic matter content	Alkali- aggregate reaction
NCA	2941	1749	10.3	1.33	0.72	0.8	Qualified	Qualified
RCA	2536	1467	14.8	7	1.86	3.02	Qualified	Qualified
Normative Value	≥2500	≥1300	≤16	–	≤1.0	–	Qualified	Qualified
Sand	2764	1830	12	2.12	1.2	4.1	Qualified	Qualified
IOT	2745	1824	19.53	8.7	2.9	1.45	Qualified	Qualified
Normative Value	–	–	≤10	–	≤3.0	–	Qualified	Qualified

(RAC-7, RAC-8) with a large amount of tailings were lower than that of the RAC-1, while the strength values (RAC-4) with a certain amount of tailings were higher than that of the NAC. From Fig. 4 (b), the influence of the carbonation period on the strength was similar to that of the curing age. Additionally, the tailings had a certain activity and a considerable influence on the later strength of the RAC and the carbonation strength.

The strength growth rate is defined as the ratio of the strength growth value at the same age to the strength of natural curing age, as shown in Fig. 5. The carbonization improved the compressive strength of the RAC, and facilitated a rise in the strength value with no obvious regular rules. For example, for an intensity value of 7 d, the growth rate of the RAC-4 was at the boundary, when the dosage was lower than 30%, the growth rate decreased, and when the dosage was higher, the opposite effect appeared. However, for other ages, the intensity values fluctuated to different degrees.

The reason for this phenomenon was that the iron tailings particles were finer and the filling effect was obvious. A small admixture amount could improve the homogeneity and compactness of concrete, increase the compressive strength and carbonization resistance (Cheng et al., 2019). An enhancement was also seen that when the dosage was 30%, and the tailings exhibited the best filling effect, the highest compressive strength. However, when the dosage was high, a large amount of iron tailings replaced the fine aggregates, which caused the aggregate gradation to be unreasonable, and the amount of concrete defects increased, thereby reducing the compressive strength value. In addition, iron tailings had “pozzolanic activity”, which promoted cement hydration (Uchechukwu and Ezekiel, 2014). Under the same conditions, the ability to consume $Ca(OH)_2$ became stronger, which reduced the alkalinity of the concrete. That is, more $Ca(OH)_2$ particles were converted into $CaCO_3$, which improved the concrete compactness and the compressive strength after carbonization (Vijayaraghavana et al., 2017). Therefore, the cubic compressive strength of the IOT-

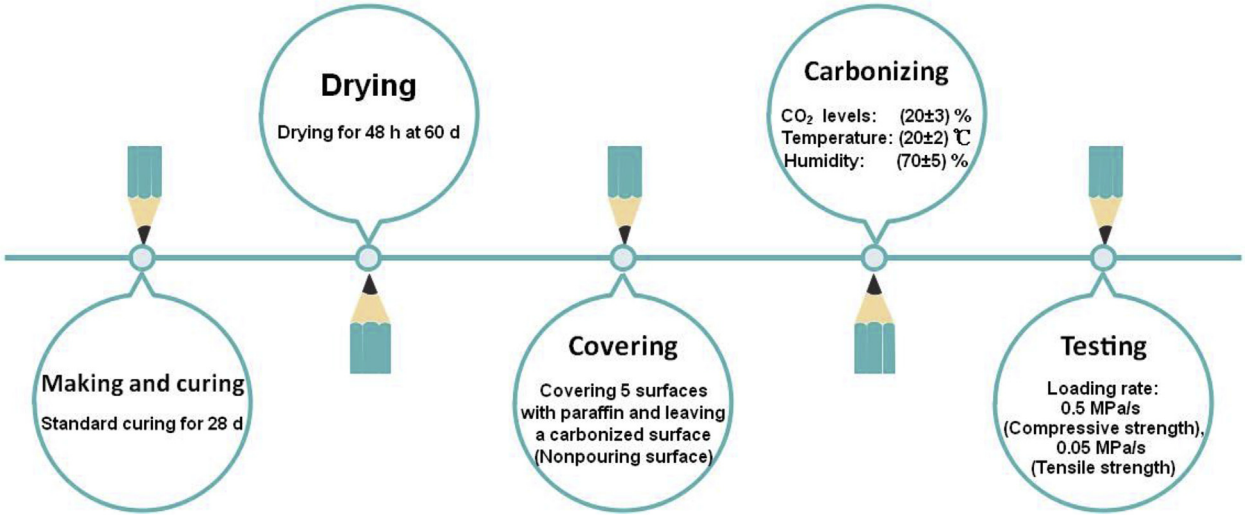

Fig. 3. Flow chart of the carbonization test.

Table 4
Mix proportion design of tailings recycled concrete under different conditions (kg/m^3).

Serial number	Block number	Cementitious materials	Coarse aggregate		Fine aggregate		Water	Substitution rate of tailings(%)
			NCA	RCA	Sand	IOT		
1	NAC	538	1063	0	572	0	215	0
2	RAC-1	538	735	315	566	0	215	0
3	RAC-2	538	739	317	512	57	215	10
4	RAC-3	538	743	319	458	114	215	20
5	RAC-4	538	744	319	402	172	215	30
6	RAC-5	538	751	322	343	229	215	40
7	RAC-6	538	755	324	290	290	215	50
8	RAC-7	538	763	327	176	410	215	70
9	RAC-8	538	773	331	0	594	215	100

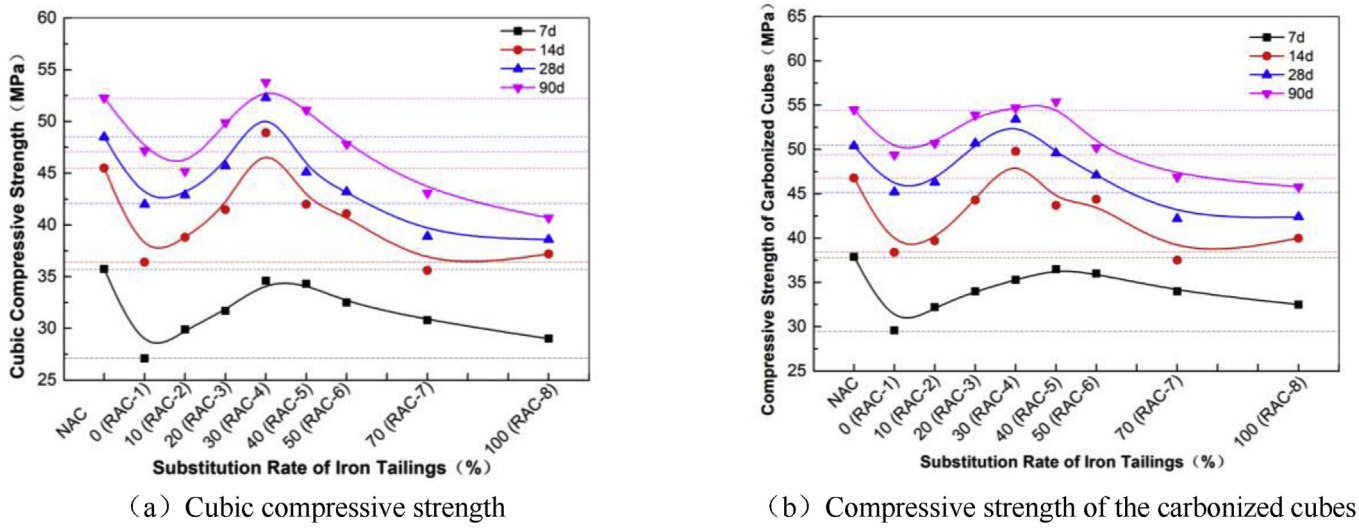

（a）Cubic compressive strength （b）Compressive strength of the carbonized cubes

Fig. 4. Relative change rate of the cubic compressive strength before and after carbonization.

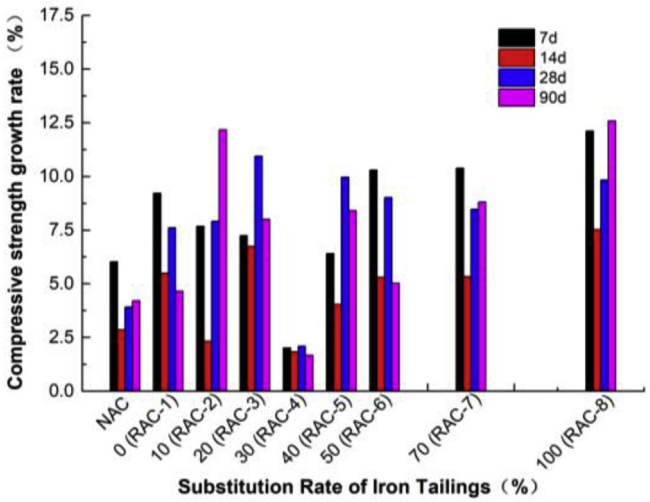

Fig. 5. Increase rate of the compressive strength after carbonization.

RACs mainly depended on the tailings filling effect and the pozzolanic activity effect. The former made the concrete more compact and increased the carbonization resistance. The latter promoted the hydration reaction, reduced the alkalinity of the concrete, and weakened the carbonation resistance.

4.2. Cubic splitting tensile strength

The splitting tensile strength of cubes was also an important index for measure the mechanical properties of concrete. Fig. 6 shows the variation curve of the cubic splitting tensile strength with the tailings substitution rate at different ages before and after carbonization.

From the above figure, with an increase in the curing age and carbonization age, the overall splitting tensile strength tended to increase. However, the increase was small, the curve remained relatively smooth, which showed the same trend as that in the literature (Chinnappa and Karra, 2020). Under the same natural curing age, the tensile strength of the concrete first increased and then decreased with the addition of tailings, however, at different curing ages, the positions of the peak points were different. At 7 d, 14 d, 28 d and 90 d, the amount of the IOTs corresponding to the position of the maximum splitting tensile strength was 30%, 20%, 40% and 40%, respectively. At this moment, the optimal mixing ratio given in the literature (Shettima et al., 2016; Wei et al., 2019) was 25% and 30%, and the increase gradually slowed down afterwards. Carbonation made the change in the tensile strength more complex, which fluctuated to varying degrees, but it could be determined that the first peak point occurred between 20% and 40%. As the carbonation age increased, the carbonization intensity also showed relatively large fluctuations, but the overall change was small and relatively gentle.

Fig. 7 shows that carbonization increased the tensile strength of most concrete samples to varying degrees, but the increase was small, and some of them also presented negative growth. The influence of tailings on concrete with a low carbonization period was relatively large, but it was smaller when the carbonization period was longer. For example, when the content was 100%, the strength increment values were 10.79% (7 d), 6.65% (14 d), 5.97% (28 d) and 1.22% (90 d), which are smaller than 20.5% (7 d) and 7.7% (28 d) (Shettima et al., 2016), also smaller than 22.8% (Ugama and Ejeh, 2014). As the carbonization time increased, the carbonized products gradually filled the pores in the concrete, thus reducing the influence degree of carbonization. Therefore, carbonization caused the cube splitting tensile strength to fluctuate, and the tailings substitution rate corresponding to the first peak was 20%–40%.

4.3. Axial compressive strength

The compressive strength of prisms with respect to carbonization for 28 d and 90 d was studied, as shown in Fig. 8.

Under natural curing and carbonation conditions, the influence of iron tailings on the axial compressive strength of concrete increased first and then decreased. Compared with the axial compressive strength, the amount of admixture at the peak point was not obvious, but the peak point was still approximately in the range of 20%–40%, which was the same as the general trend of the relevant literature, with the optimal amount of tailings being 60% (Xu, 2019). As shown in Fig. 8(a), when the content of tailings was lower (<30%), the effect of carbonation on the axial compressive strength of RAC was more obvious. At 90 d of natural curing, the pressure decreased slightly after the peak point (20%–40%) and then increased gradually, while at 90 d after carbonization, the peak

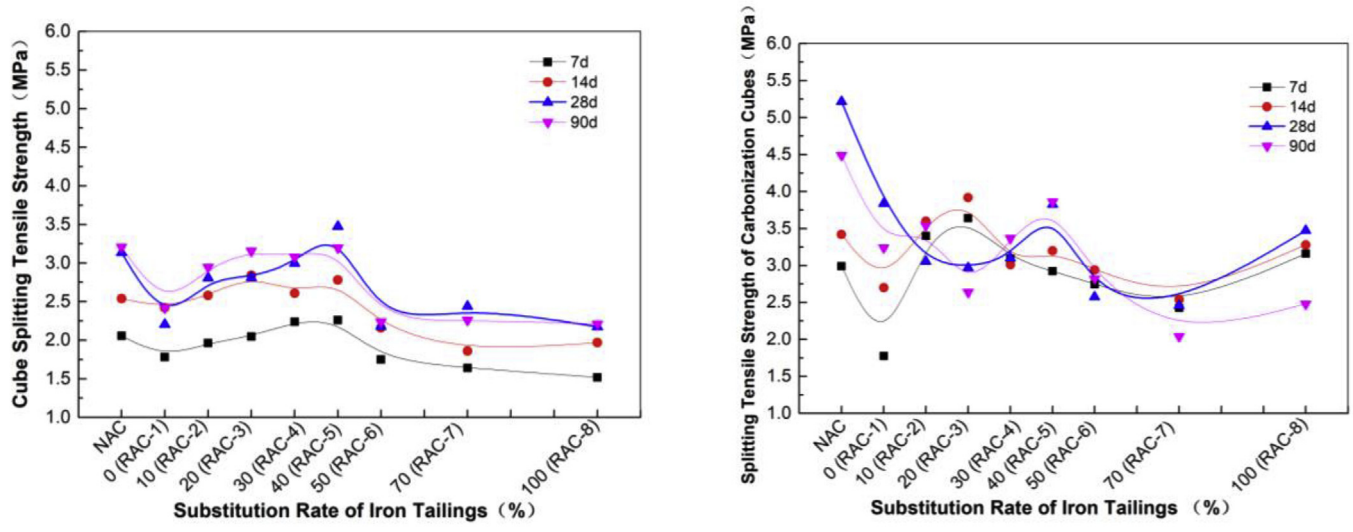

（a）Splitting tensile strength （b）Splitting tensile strength after carbonization

Fig. 6. Relative change rate of the splitting tensile strength before and after carbonization.

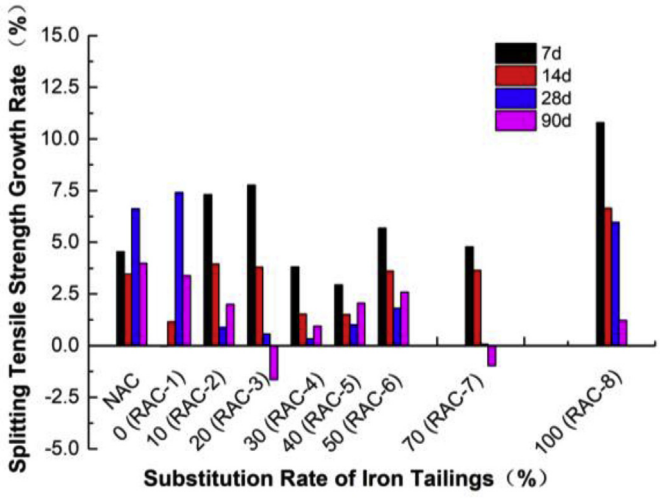

Fig. 7. Increase rate of the splitting tensile strength after carbonization.

point was relatively flat. Therefore, it could be predicted that with increasing time, the hydration degree of cement will gradually improve (Evangelista and de Brito, 2007), and the strength difference under axial compression will gradually decrease with the different tailings contents (Shettima et al., 2016). From Fig. 8(b), under long term action, the intensity growth rate generated by carbonization gradually decreased and finally emerged as negative growth (RAC-7, RAC-8). However, the unreasonable gradation caused by excessive tailings still existed, so the strength value of the later period had changed. The reason lies in the micro-powder effect and the activity of iron tailings, which made the microstructure and chemical composition of the concrete change slightly (Sharma and Khan, 2017).

4.4. Deformation performance

The deformation properties of concrete mainly included the peak strain and elastic modulus. The specific test values are shown in Table 5, and the corresponding change rates are shown in Fig. 9 and Fig. 10.

Fig. 9 shown that the overall trends of the different carbonization cycles and tailings dosage were the same, regardless of the peak strain and elastic modulus. On the whole, when the initial mixing amount was small (≤40%), the tailings caused the peak strain of the IOT-RAC to change irregularly, with the peak point appearing in the range of 10%–40%. This phenomenon was similar to that observed in the literature (Xu, 2019), which showed that the optimum dosage was 20%. Finally, when the amount was large, the peak strain value changed approximately linearly, and the longer the carbonization cycle was, the slower the rate of change was. At the same time, the peak strains of the RAC at all admixtures were better than those of the RAC-1, while its values of most admixtures were better than those of ordinary concrete, which also indicated that carbonization could improve the peak strain of the IOT-RAC. According to Fig. 10, the influence rule of carbonization and tailing content on the elastic modulus of the RAC were similar to that of the peak strain, which also caused a greater fluctuation of its value, and the peak point appeared in the range of 20%–40%. This result was also observed by Thomas et al. (2013), whose results showed that the value of elasticity modulus gradually increase until 30%, 60% and 0% substitution with varying water-cement ratios of 0.4, 0.45 and 0.5, respectively.

When the tailings content was small (≤20%), during the same carbonization period, different degrees of fluctuations occurred. The largest deformation performance was exhibited after approximately 28 d. For example, the peak strain of carbonized 28 d (RAC-1) remained 36.9% higher than that of carbonized 0 d. Compared with 0 d, the elastic modulus of NAC and RAC-3 increased by 58.6% and 34.9% after 28 d, respectively. When the tailings content was large (>20%), with increasing carbonization age, the deformation properties of each tailings samples exhibited the same trend: 0 d > 28 d > 90 d. The results also showed that the peak strain and elasticity modulus of the concrete could be reduced to some extent by adding tailings, which directly led to a reduction in the compressive strength (Figs. 4 and 6).

4.5. Stress-strain constitutive curve

The stress-strain curve measurement in this paper uses the MTI-

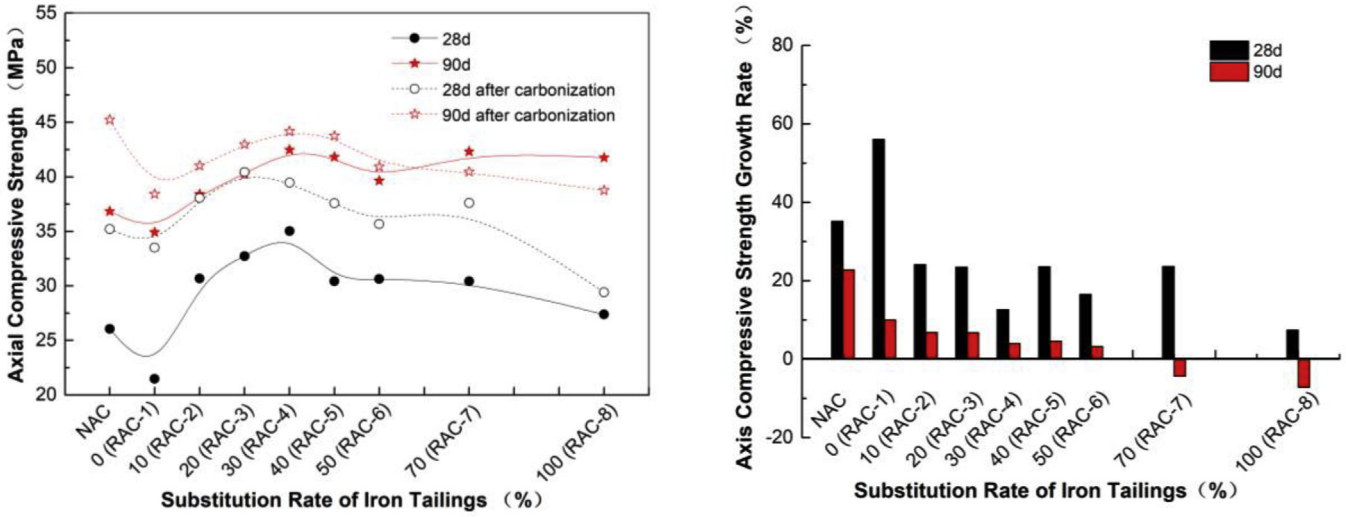

（a）Axial compressive strength （b）Increase rate of axis compressive strength

Fig. 8. Relative change in the axial compressive strength before and after carbonization.

3D noncontact strain measurement system to simultaneously perform data acquisition with the microcomputer controlled electrohydraulic servo universal testing machine. The typical failure mode of the test blocks ars shown in Fig. 11.

Table 5
Main eigenvalues of the experimental constitutive curves.

Specimen number	σ_0/MPa			ε_0/($\times 10^{-3}$)			E_0/($\times 10^4$ MPa)		
	0d	28d	90d	0d	28d	90d	0d	28d	90d
NAC-11	26.71	34.82	45.24	2.76	3.152	2.69	0.95	1.51	1.25
RAC-1	21.47	33.51	38.42	2.02	2.766	2.31	0.98	1.03	1.28
RAC-2	31.67	38.07	41.63	3.15	3.38	2.56	1.42	1.59	1.07
RAC-3	32.73	40.83	42.97	2.81	2.688	3.33	0.99	1.34	1.29
RAC-4	35.04	39.48	44.18	3.27	3.05	2.93	1.53	1.47	1.39
RAC-5	32.41	36.60	43.75	3.54	3.29	2.77	1.42	1.71	1.27
RAC-6	30.62	35.68	40.94	2.79	2.738	2.61	1.17	1.09	1.02
RAC-7	30.41	37.62	40.47	3.07	2.914	2.49	1.34	1.30	1.09
RAC-8	27.38	29.41	39.76	3.95	2.84	2.61	1.68	1.31	1.15

Remarks: The data were the average values of specimens, and the dispersion was no more than 10% in accordance with the specifications. The parameters σ_0 and ε_0 are the peak stress and peak strain, respectively. E_0 represents the initial elastic modulus of concrete, approximating the secant modulus when $\sigma_c = 0.4\ \sigma_0$.

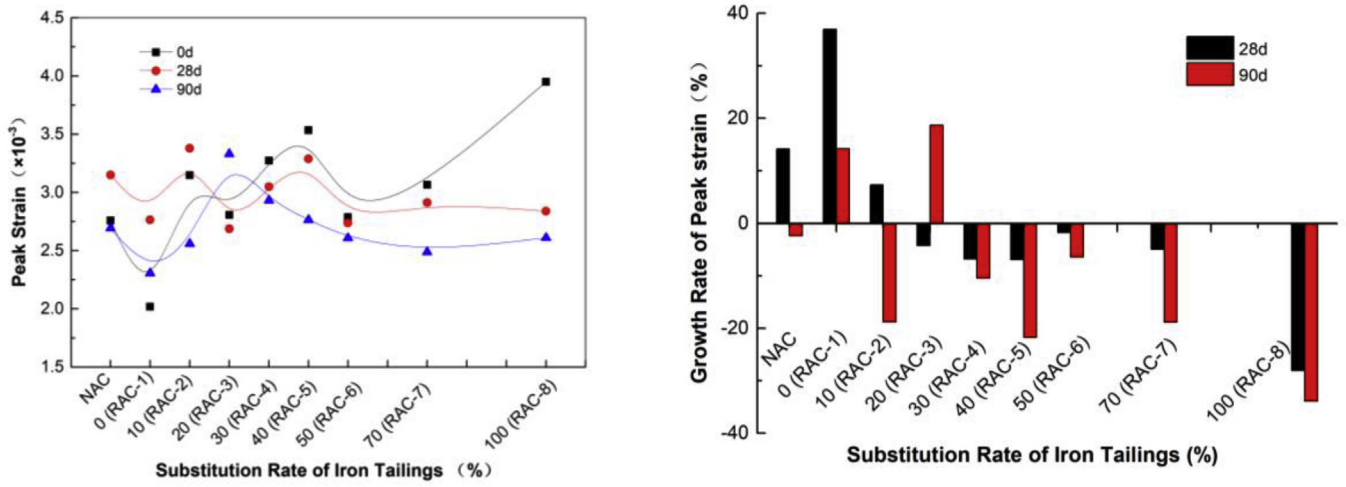

（a）Peak strain （b）Increase rate of the peak strain

Fig. 9. Relative change rate of the peak strain before and after carbonization.

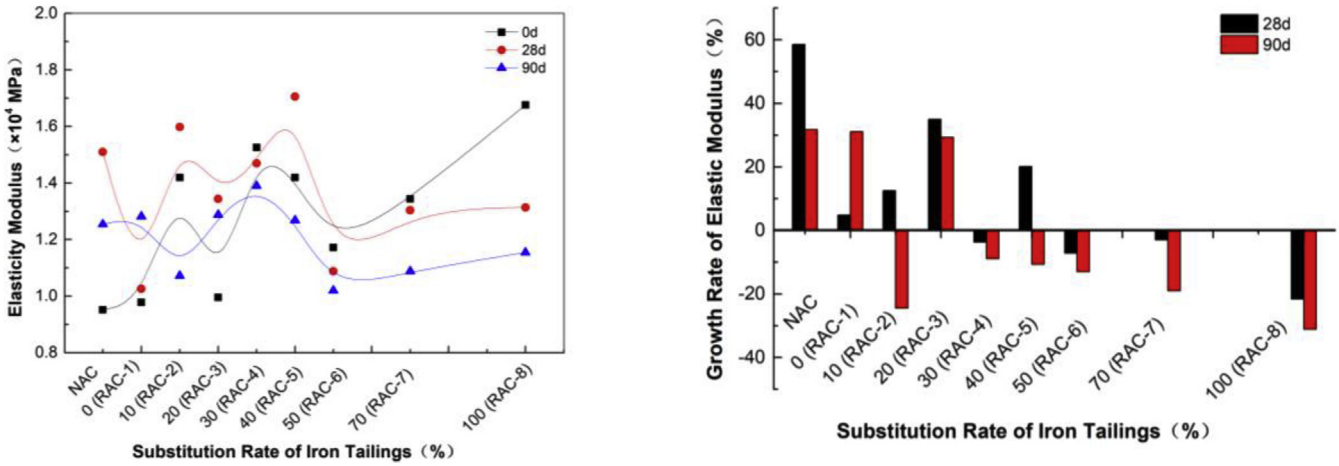

(a) Elasticity modulus (b) Increase rate of the elasticity modulus

Fig. 10. Relative change rate of the elasticity modulus before and after carbonization.

The formation, gradual development, and finally intersection of micro-cracks demonstrates the process of compressive failure of prism specimens (Thomas et al., 2019; Xu et al., 2016). At the initial loading stage, the strain increased approximately proportionally, and the test block was in an elastic stage with no cracks. As the load continued to increase and the whole body entered the elastic-plastic stage, the stress-strain curve was convex, and the internal micro-cracks gradually occurred. Until the peak strain, there was no significant difference between the carbonized and non-carbonized specimens. Due to the frictional force, when approaching the peak strain, a small number of vertical cracks appeared at the upper and lower ends of the test block surface. After crossing the peak point, the concrete at the end of the test block crushed and began to fall off, and the cracks gradually extended and intersected. Most of the blocks with tailings eventually formed an oblique main crack and underwent vertical shear failure. The longer the carbonization cycle was, the higher the tailings content was, the more sudden the crack formation was, the greater the mount of concrete that fell off after the test was, and the brittleness was more obvious.

The stress-strain curves of carbonization for 0 d (natural curing for 28 d), 28 d and 90 d are shown in Fig. 12.

The above figures show that there were no essential difference in the shape of the stress-strain curve before and after carbonization. The variation range of the ascending section was relatively small, while that of the descending section was relatively large, which indicated that carbonation and tailings content had a more obvious influence on the descending section of the concrete. On the whole, it could be approximated that the larger the tailings content was, the more sudden the deformation of the descending section was, and the steeper the falling section was. Similar results were also observed by Wang et al. (2019) and Asprone et al. (2014). At the same time, the ascending section showed an unstable development

(a) NAC (0 d) (b) NAC (90 d) (c) RAC-8 (0 d) (d) RAC-8 (90d)

Fig. 11. Typical failure modes of the specimens before and after carbonization.

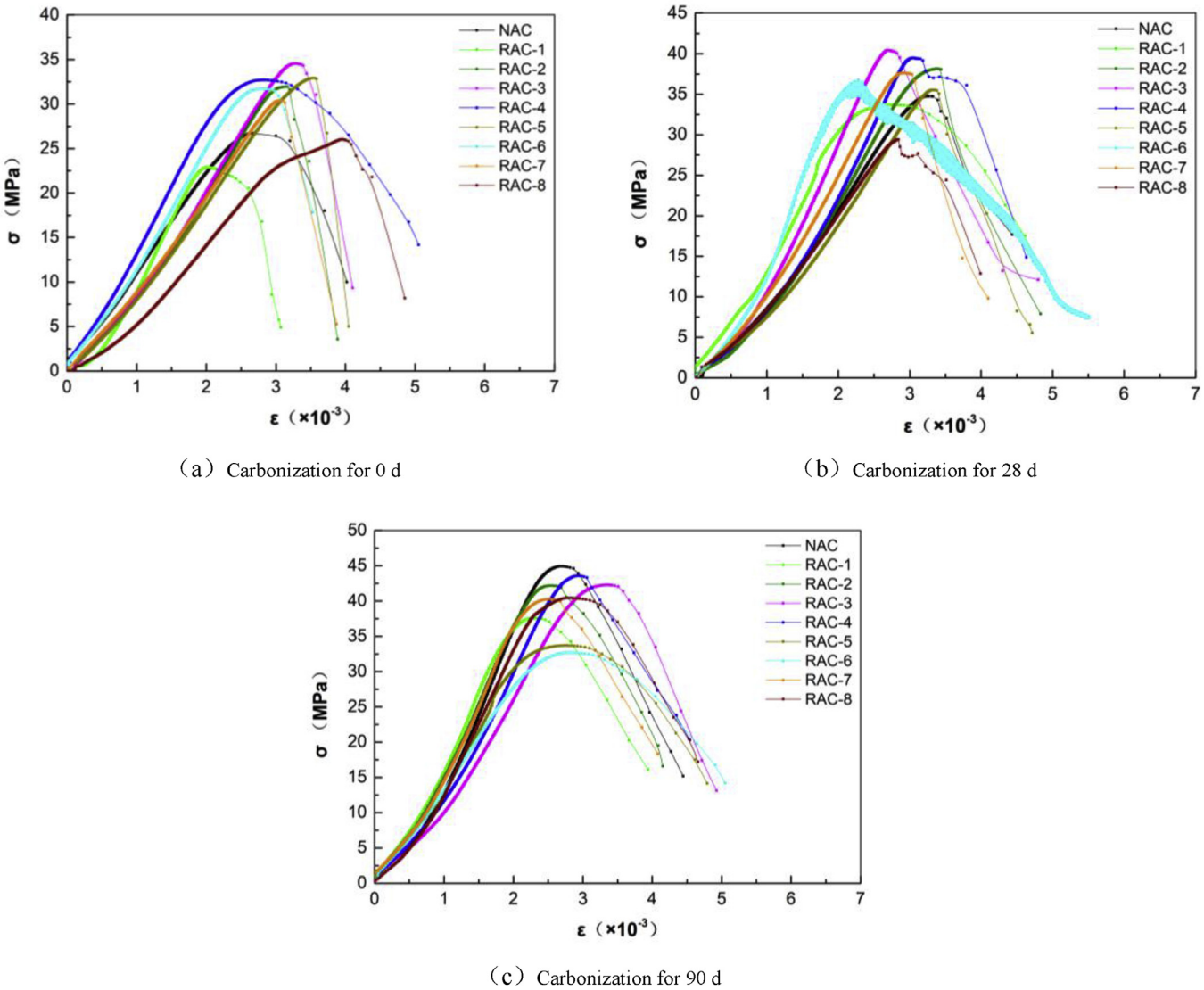

Fig. 12. Effect of carbonization on the stress-strain curve.

trend. The longer the carbonization cycle was, the lower the dispersion of the stress-strain curve of the IOT-RAC was. Additionally, the cycle finally was stable, that is, the ascending section gradually tended to shrink, and the trend of each descending section gradually became uniform.

This behavior was mainly because the mechanical properties of concrete often depended on the compactness of the concrete, the state of the internal pores and the development of cracks (Du and Wang, 2016; Li et al., 2019). The longer the carbonation period was, the more perfect the hydration of cementitious materials was, the higher the degree of carbonation was, the stronger the compactness of the concrete was, and the greater the improvement in the internal pores was. Simultaneously, the crack in the ascending section had not appeared or appeared less, so the ascending section curve was gradually gathered. However, a large number of cracks appeared in the descending stage with a strong randomness. Due to the release of a large amount of strain energy in the descending section, it developed rapidly, which brought a new difficulty to the test. Over all, it was still consistent with the variation characteristics of the entire stress-strain curve of concrete materials (Guo, 2014).

5. Deterioration mechanism analysis of carbonization on the IOT-RAC

The concrete strength was mainly generated by the hydration of cementitious materials to produce corresponding new substances. It was necessary to analyze the hydration process and products (Gao and Wu, 2018). Therefore, EDS and SEM were used to analyze the microstructure, to determine the carbonization damage and deterioration mechanism of recycled concrete. Fig. 13 and Table 6 show the typical test results of EDS when carbonized for 0 d.

Due to the different sweeping angles of the selected samples, except for a slightly larger increment in the carbon content, the other individual elements showed a slight change under different carbonization cycles. The content of Al and Si (RAC) is the lowest. After the tailings were mixed (RAC-8), the content was increased by a factor of 2.27 and 78%, and the effect proved to be more obvious. This finding also showed that the hydration degree of concrete was relatively higher. After hydration, the quantity of calcium silicate hydrate (C–S–H), monosulfate hydrated calcium sulfoaluminate (AFm) and trisulfide hydrated calcium sulfoaluminate (AFt) significantly increased.

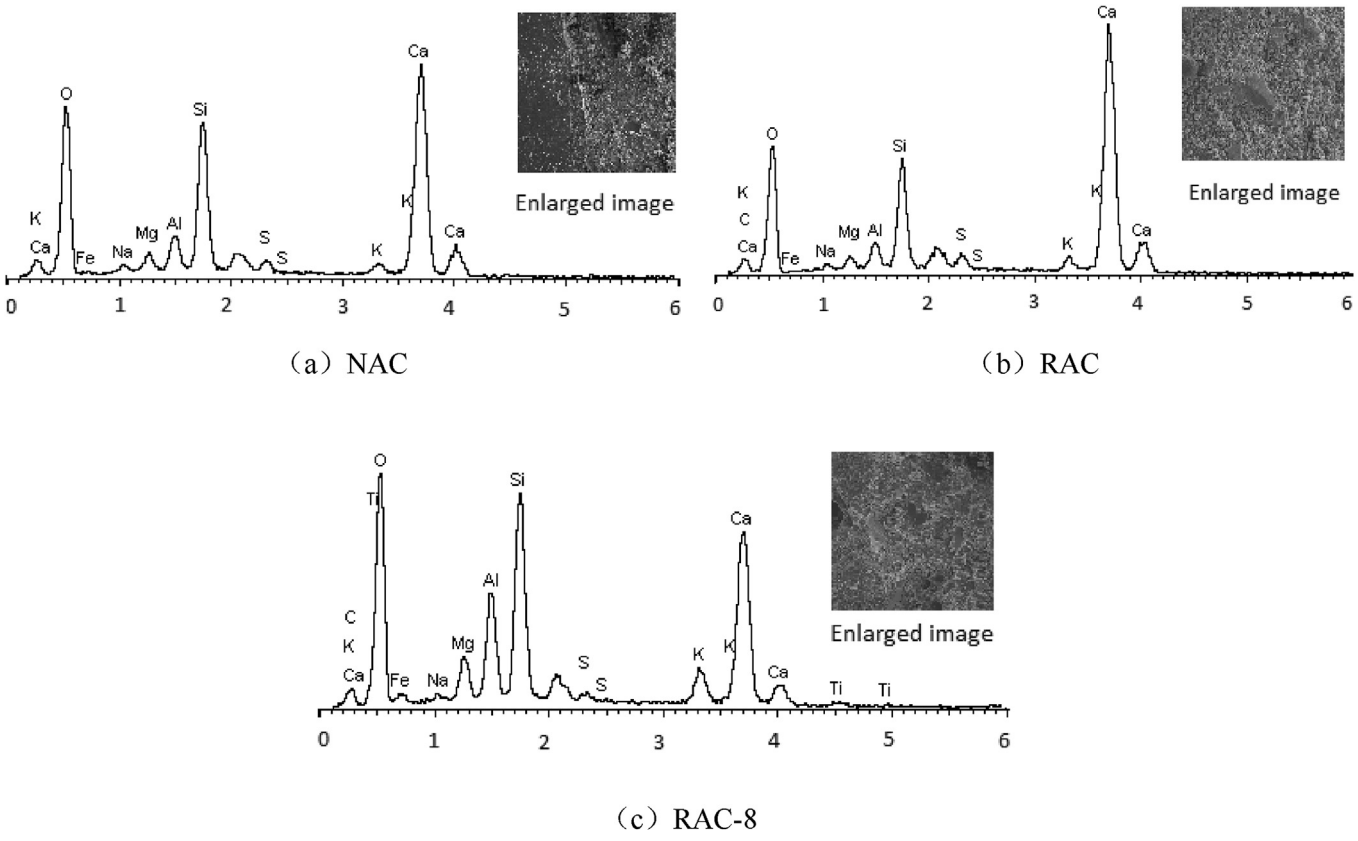

Fig. 13. EDS atlas analysis (0 d).

Table 6
Main chemical compositions(0 d).

Mineral Composition		O	Na	Mg	Al	Si	S	K	Ca	Fe	Others
Content(%)	NAC	56.86	0.42	0.97	1.91	9.13	1.03	1.07	27.53	1.08	0
	RAC	51.62	0.36	0.67	1.37	6.82	1.27	1.27	33.53	0.40	2.69
	RAC-8	52.14	0.3	1.09	4.48	12.15	0.52	1.73	17.84	2.40	7.35

Fig. 14 illustrated a typical SEM test results of the IOT-RAC before and after carbonization. Referring to the relevant literatures (Zhang et al., 2015; Yuan et al., 2013) and combined with the common morphology of hydration products, we can confirm the material composition in its microstate.

5.1. Influence of the tailings content on the microstructure

From the chemical composition analysis in the above figures, whether it was the NAC, RAC or IOT-RAC, $Ca(OH)_2$ of plate-like materials and ettringite of spicules or rods can be clearly seen before carbonization, but the content was different. The NAC (Fig. 14(a)) and RAC-1 (Fig. 14(c)) contained a large number of plate-like substances ($Ca(OH)_2$), while the spicule-like and rod-like substances were less, which indicated a weak degree of hydration. After the addition of the tailings (Fig. 14(e) and (g)), there were obvious needle-like, rod-like, and intertwined clusters of ettringite, which also indicated that the tailings exhibited a certain activity to promote the hydration of concrete and promoted the development of concrete relatively perfect (Bonaccorsi et al., 2005; Ma et al., 2016). The higher the content of tailings was, the more acicular and bar-like the products were, the more perfect the development of concrete was, which corresponded to the improvement in its mechanical properties(Figs. 4, 6 and 8). However, the higher the content of the tailings was, the more the harmful pores and cracks in the microstructure were, and the worse the mechanical properties were. Therefore, it was necessary to strictly control the amount of tailings incorporation, to avoid the occurrence of excessive content and performance deterioration.

From the degree of the matrix structure density analysis, through Fig. 14(a) and (c), due to an increase in the ITZ between the old mortar and aggregate (Shi et al., 2016), the new mortar and aggregate, the old mortar and the new mortar, the addition of recycled aggregates directly led to the existence of more cracks between the different materials, and a looser matrix structure. Combined with Fig. 14(e) and (g), the fine powder effect of the tailings could improve the ITZ of the RCA, reducing the number of cracks and the corresponding length and width (Gao et al., 2005). Simultaneously, the addition of tailings could facilitate needle-like and rod-like ettringite formations. The larger the content of tailings was, the greater the volcanic ash activity effect was, which could promote the cementitious materials hydration (Han et al., 2019). However, the addition of excessive tailings deteriorated the mix ratio of concrete, reduced the integrity of the matrix structure, and produced various staggered hydration products. Intuitive performance displayed that there were many holes and loose matrix

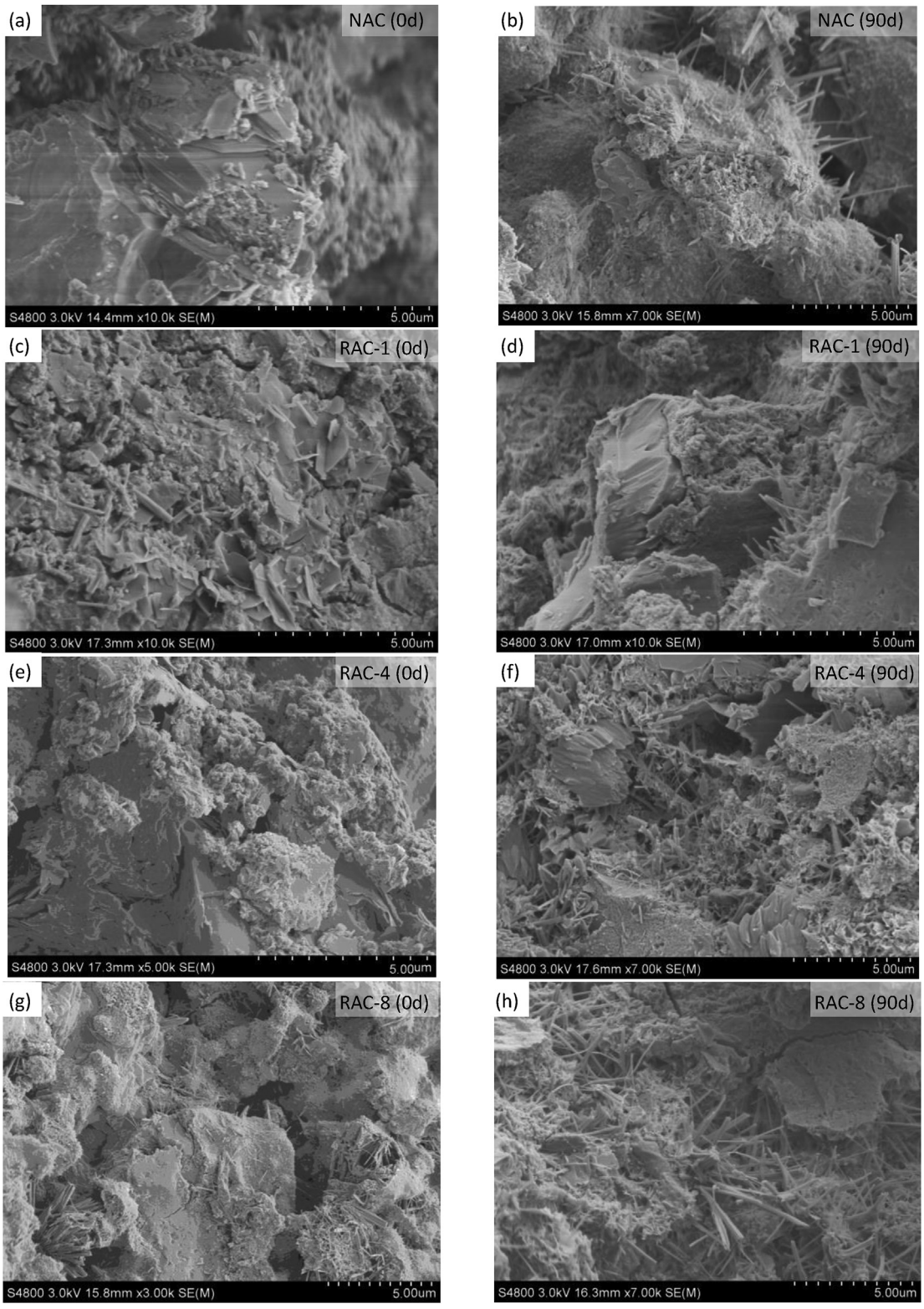

Fig. 14. SEM morphology of (a) NAC(0d); (b)NAC(90d); (c)RAC-1(0d); (d)RAC-1(90d); (e)RAC-4(0d); (f)RAC-4(90d); (g)RAC-8(0d); and (h)RAC-8(90d).

structures (Fig. 14(g)), which were bound to affect the mechanical properties of the material.

5.2. Influence of carbonization on the microstructure

Compared with non-carbonization, the intuitive phenomenon of carbonization was that the ITZ of the RAC was improved, the number and width of micro-cracks were alleviated (Fig. 14(d)). Additionally, the ettringite content was significantly higher than that of the left side, indicating that the carbonization made the hydration of the cementitious material more perfect, which was also consistent with the mechanism of carbonization, including a

series of physical and chemical reactions:

$$CO_2 + H_2O \rightarrow H_2CO_3 \quad (1)$$

$$C-H + H_2CO_3 \rightarrow CaCO_3 + H_2O \quad (2)$$

$$C-S-H + CO_2 \rightarrow CaCO_3 + SiO_2 + H_2O \quad (3)$$

When the tailings content was large, carbonization destroyed the concrete matrix structure, where a large number of dry-shrinkage micro-cracks appeared (Fig. 14(e)). The former was mainly due to CO_2 entering the concrete along the crack and carbonizing reaction with $Ca(OH)_2$ (Li et al., 2018). The generated $CaCO_3$ filled the gap and optimized the ITZ of the RAC, which improved the compactness of the concrete and increased the strength after carbonization (Xu et al., 2018). The latter was mainly due to the addition of a large amount of tailings. On the one hand, it promoted the hydration reaction of concrete and needed to consume part of free water. On the other hand, the growth of the carbonized product $CaCO_3$ in stress-free zones, such as cracks and pores, also needed to consume the hydration product $Ca(OH)_2$ and free water in stress zones at the cost, which caused the shrinkage of the cement paste. When the shrinkage was limited, tensile stress occurred, and tension cracks appeared (Kashef-Haghi et al., 2015).

In summary, tailings particles exhibited the characteristics of "pozzolanic activity" and "fine powder". A proper tailings content (20%–40%) could fill harmful pores, promote the hydration of cementitious materials and improve the ITZ of the RAC. However, when the amount of tailings was large, the tailings particles changed the aggregate particle gradation to some extent, resulting in an increase in harmful voids in the matrix structure, which affected the corresponding mechanical properties of the concrete. After carbonization, concrete with less tailings (<40%) could fill harmful voids in the concrete matrix, improve the compactness of the concrete and the corresponding mechanical properties. Conversely, when the tailings amount was large, the accumulation of tailings activity and the intensification of the carbonization reaction increased the consumption of free water, and generated a large number of dry shrinkage cracks, which reduced the corresponding mechanical properties.

6. Conclusions

By analyzing the macroscopic mechanical properties and microstructure of the IOT-RAC before and after carbonization, the following conclusions can be drawn:

(1) Most of the mechanical property indexes of the IOT-RAC increased with the addition of a small amount of tailings, but decreased with the addition of excessive tailings. Before carbonization, the peak values of the cubic compressive strength, splitting tensile strength and axial compressive strength were 30%, 30%, 20%–40%, respectively. After carbonization, the strength value of each corresponding age increased to different degrees, but the overall rule was similar to the situation before carbonization, and the optimal mixing amount was: 30%, 20%–40% and 20%–40%, respectively.

(2) With the addition of the tailings, the peak strain and elastic modulus of IOT-RAC showed a similar trend before and after carbonization. Macroscopically, the tailings amount had little effect on the ascending section of the stress-strain curve, showing a similar trend to cement-based materials before and after carbonization. Due to the randomness of the cracks, there were large fluctuations in the descending section. However, as a whole, it could be approximated that the larger the tailings content was, the stronger the brittleness of the concrete was and the steeper the falling section was.

(3) Through EDS and SEM analysis, the chemical composition and matrix structure of the recycled concrete were analyzed at the microscopic level of the tailings content and carbonization. The macroscopic mechanical properties were verified, and a performance degradation mechanism was proposed.

From macroscopic and microscopic analyses, it can be confirmed that the appropriate amount of tailings can fill the harmful pores and cracks in the matrix structure, and promote the hydration of cementitious materials, improve the compactness of recycled concrete and its mechanical properties. On the whole, the optimum dosage is 20%–40%, to give full play to the value of resources and obtain the most favorable effect.

Author contribution statement

Tao Li: Conceptualization, Methodology, Formal analysis, Writing - Original Draft.

Sheliang Wang: Conceptualization, Writing - Review & Editing.

Fan Xu: Methodology, Formal analysis, Data Curation, Writing - Review & Editing.

Xiangyin Meng: Software, Validation.

Binbin Li: Software, Resources.

Meng Zhan: Resources, Investigation.

Declaration of competing interest

The authors declare that they have no known competing financial interests or personal relationships that could have appeared to influence the work reported in this paper.

Acknowledgements

This work was funded by the National Natural Science Foundation of China (NO. 51678480); Henan province key projects of science and technology (192102310277, 182102310834); Shaanxi Provincial Science and Technology Department Key Scientific Research Project(2018GY-099, S2018-YF-YBGY-0149); Scientific Research Project of Key Laboratory of Shaanxi Education Department (17JS071); Scientific Research Projects of Shaanxi Education Department (18JK0248), Shangluo science and Technology Bureau Project (SK2016-50).

References

Cui, H.H., Yang, X., Hu, J.L., Zhang, Z.G., Yao, S.J., 2018. Study on the matching and mechanical properties of regenerated concrete with iron tailings. Sichuan Build. Sci. 44 (5), 100–105. https://doi.org/10.19794/j.cnki.1008-1933.2018.05.019.

Albayati, A., Wang, Y., Wang, Y., Haynes, J., 2018. A sustainable pavement concrete using warm mix asphalt and hydrated lime treated recycled concrete aggregates. Sustain. Mater. Technol. 20, e00081 https://doi.org/10.1016/j.susmat.2018.e00081.

Asprone, D., Cadoni, E., Iucolano, F., Prota, A., 2014. Analysis of the strain-rate behavior of a basalt fiber reinforced natural hydraulic mortar. Cement Concr. Compos. 53, 52–58. https://doi.org/10.1016/j.cemconcomp.2014.06.009.

Bonaccorsi, E., Merlino, S., Kampf, A.R., 2005. The crystal structure of tobermorite 14Å (Plombierite), aC-S-H phase. J. Am. Ceram. Soc. 88 (3), 505–512. https://doi.org/10.1111/j.1551-2916.2005.00116.x.

Cheng, Y.H., Huang, F., Li, W.C., Liu, R., Li, G.L., Wei, J.M., 2016. Test research on the effects of mechanochemically activated iron tailings on the compressive strength of concrete. Construct. Build. Mater. 118, 164–170. https://doi.org/10.1016/j.conbuildmat.2016.05.020.

Cheng, Y.H., Huang, F., Qi, S.S., Li, W.C., 2019. Effects of high-silicon iron tailings on carbonation and Sulphate corrosion resistance of concrete. J. Northeast. Univ. (Nat. Sci.) 40 (1), 121–125+149. https://doi.org/10.12068/j.issn.1005-3026.2019.01.023.

Chinnappa, G.B., Karra, R.C., 2020. Experimental and statistical evaluations of strength properties of concrete with iron ore tailings as fine aggregate. J. Hazard. Toxic Radioact.Waste 24 (1). https://doi.org/10.1061/(ASCE)HZ.2153-5515.0000480, 04019038.

Dandautiya, R., Singh, A.P., 2019. Utilization potential of fly ash and copper tailings in concrete as partial replacement of cement along with life cycle assessment. Waste Manag. 99, 90–101. https://doi.org/10.1016/j.wasman.2019.08.036.

Du, Y.F., Wang, S.L., 2016. Experimental study on seismic behavior of FR-RAC beam-column joints. J. Build. Struct. 37 (4), 40–46. https://doi.org/10.14006/j.jzjgxb.2016.04.006.

Evangelista, L., de Brito, J., 2007. Mechanical behaviour of concrete made with fine recycled concrete aggregates. Cement Concr. Compos. 29 (5), 397–401. https://doi.org/10.1016/j.cemconcomp.2006.10.004.

Ferreira, L., de Brito, J., Barra, M., 2011. Influence of the pre-saturation of recycled coarse concrete aggregates on concrete properties. Mag. Concr. Res. 63 (8), 617–627. https://doi.org/10.1680/macr.2011.63.8.617.

Gao, C.M., Wu, W.J., 2018. Using ESEM to analyze the microscopic property of basalt fiber reinforced asphalt concrete. Int. J. Pav. Res. Technol. 11, 374–380. https://doi.org/10.1016/j.ijprt.2017.09.010.

Gao, J.M., Qian, C.X., Liu, H.F., Wang, B., Li, L., 2005. ITZ microstructure of concrete containing GGBS. Cement Concr. Res. 35, 1299–1304. https://doi.org/10.1016/j.cemconres.2004.06.042.

Goyal, S., Singh, K., Hussain, A., Singh, P.R., 2015. Study on partial replacement of sand with iron ore tailing on compressive strength of concrete. Int. J. Res. Eng. Adv. Technol. 3 (2), 243–248.

Gu, S., 2019. Basic Properties and Engineering Application of Recycled Concrete. Wuhan University Press, Wuhan.

Guo, Z.H., 2014. Principles of Reinforced Concrete. Tsinghua University Press, Beijing.

Han, F.H., Song, S.M., Liu, J.H., Huang, S., 2019. Properties of steam-cured precast concrete containing iron tailing powder. Power Technol. 345, 292–299. https://doi.org/10.1016/j.powtec.2019.01.007.

Kashef-Haghi, S., Shao, Y., Ghoshal, S., 2015. Mathematical modeling of co_2 uptake by concrete during accelerated carbonation curing. Cement Concr. Res. 67, 1–10. https://doi.org/10.1016/j.cemconres.2014.07.020.

Kox, S., Vanroelen, G., Van Herck, J., de Krem, H., Vandoren, B., 2019. Experimental evaluation of the high-grade properties of recycled concrete aggregates and their application in concrete road pavement construction. Case Stud. Constr. Mater. 11, e00282 https://doi.org/10.1016/j.cscm.2019.e00282.

Li, W.S., Lei, G.Y., Xu, Y., Huang, Q.F., 2018. The properties and formation mechanisms of eco-friendly brick building materials fabricated from low-silicon iron ore tailings. J. Clean. Prod. 204, 685–692. https://doi.org/10.1016/j.jclepro.2018.08.309.

Li, H.N., Liu, P.F., Li, C., Li, G., Zhang, H., 2019. Experimental research on dynamic mechanical properties of metal tailings porous concrete. Construct. Build. Mater. 213, 20–31. https://doi.org/10.1016/j.conbuildmat.2019.04.049.

Lu, H.J., Qi, C.C., Chen, Q.S., Gan, D.Q., Xue, Z.L., Hu, Y.J., 2018. A new procedure for recycling waste tailings as cemented paste backfill to underground stopes and open pits. J. Clean. Prod. 188, 601–612. https://doi.org/10.1016/j.jclepro.2018.04.041.

Lu, B., Shi, C.J., Cao, Z.J., Guo, M.Z., Zheng, J.L., 2019. Effect of carbonated coarse recycled concrete aggregate on the properties and microstructure of recycled concrete. J. Clean. Prod. 233, 421–428. https://doi.org/10.1016/j.jclepro.2019.05.350.

Lv, X.D., Shen, W.G., Wang, L., Dong, Y., Zhang, J.F., Xie, Z.Q., 2019. A comparative study on the practical utilization of iron tailings as a complete replacement of normal aggregates in dam concrete with different gradation. J. Clean. Prod. 211, 704–715. https://doi.org/10.1016/j.jclepro.2018.11.107.

Ma, B.G., Cai, L.X., Li, X.G., Jian, S.W., 2016. Utilization of iron tailings as substitute in autoclaved aerated concrete: physico-mechanical and microstructure of hydration products. J. Clean. Prod. 127, 162–171. https://doi.org/10.1016/j.jclepro.2016.03.172.

Ministry of Housing and Urban-Rural Construction of the People's Republic of China, 2009. Standard Fortest Methods of Long-Term Performance and Durability of Ordinary Concrete (GB/T50082-2009). China Architecture & Building Press, Beijing.

Ministry of Housing and Urban-Rural Construction of the People's Republic of China, 2011. Specification for Mix Proportion Design of Ordinary Concrete (JGJ55-2011). China Architecture & Building Press, Beijing.

Ministry of Housing and Urban-Rural Construction of the People's Republic of China, 2015. Code for Design of Concrete structures(GB/T50010-2015). China Architecture & Building Press, Beijing.

Ministry of Housing and Urban-Rural Construction of the People's Republic of China, 2018. Technical Standard for Recycled Concrete Structures (JGJ/T 443-2018). China Architecture & Building Press, Beijing.

Qi, C.C., Fourie, A., Chen, Q.S., Zhang, Q.L., 2018. A strength prediction model using artificial intelligence for recycling waste tailings as cemented paste backfill. J. Clean. Prod. 183, 566–578. https://doi.org/10.1016/j.jclepro.2018.02.154.

Sani, D., Moriconi, G., Fava, G., Corinaldesi, V., 2005. Leaching and mechanical of concrete manufactured with recycled aggregates. Waste Manag. 25 (2), 177–182. https://doi.org/10.1016/j.wasman.2004.12.006.

Shaban, W.M., Yang, J., Su, H.L., Liu, Q.F., Tsang, D.C.W., Wang, L., Xie, J.H., 2019. Properties of recycled concrete aggregates strengthened by different types of pozzolan slurry. Construct. Build. Mater. 216, 632–647. https://doi.org/10.1016/j.conbuildmat.2019.04.231.

Sharma, R., Khan, R., 2017. Durability assessment of self-compacting concrete incorporating copper slag as fine aggregates. Construct. Build. Mater. 155, 617–629. https://doi.org/10.1016/j.conbuildmat.2017.08.074.

Shettima, A.U., Hussin, M.W., Ahmad, Y., Mirza, J., 2016. Evaluation of iron ore tailings as replacement for fine aggregate in concrete. Construct. Build. Mater. 120, 72–79. https://doi.org/10.1016/j.conbuildmat.2016.05.095.

Shi, C.J., Li, Y.K., Zhang, J.K., Li, W.G., Chong, L.L., Xie, Z.B., 2016. Performance enhancement of recycled concrete aggregate: a review. J. Clean. Prod. 112, 166–472. https://doi.org/10.1016/j.jclepro.2015.08.057.

Tang, K., Mao, X.S., Xu, W., 2019. Performance analysis of cement concrete with iron tailings sand as fine aggregate. Ind. Constr. 49 (8), 153–157. https://doi.org/10.13204/j.gyjz201908025.

Thomas, B.S., Damare, A., Gupta, R.C., 2013. Strength and durability characteristics of copper tailing concrete. Construct. Build. Mater. 48, 894–900. https://doi.org/10.1016/j.conbuildmat.2013.07.075.

Thomas, C., de Brito, J., Cimentada, A., Sainz-Aja, J.A., 2019. Macro- and micro-properties of multi-recycled aggregate concrete. J. Clean. Prod. https://doi.org/10.1016/j.jclepro.2019.118843.

Tiwari, A., Singh, S., Nagar, R., 2016. Feasibility assessment for partial replacement of fine aggregate to attain cleaner production perspective in concrete: a review. J. Clean. Prod. 135, 490–507. https://doi.org/10.1016/j.jclepro.2016.06.130.

Uchechukwu, E.A., Ezekiel, M.J., 2014. Evaluation of the iron ore tailings from Itakpe in Nigeria as concrete material. Adv. Mater. 3 (4), 27–32. https://doi.org/10.11648/j.am.20140304.12.

Ugama, T.I., Ejeh, S.P., 2014. Iron ore tailing as fine aggregate in mortar used for masonry. Int. J. Adv. Eng. Technol. 7 (4), 1170–1178.

Vijayaraghavana, J., Belin Jude, A., Thivya, J., 2017. Effect of copper slag, iron slag and recycled concrete aggregate on the mechanical properties of concrete. Resour. Pol. 53, 219–225. https://doi.org/10.1016/j.resourpol.2017.06.012.

Wang, Q.Y., Dong, J.F., 2018. Material Properties and Analysis of the Recycled Aggregate Concrete Andits Confined Structures. Science Press, Beijing.

Wang, S.L., Li, T., Yang, T., Zhang, B., Ju, J., 2013. Experimental study on seismic behavior of RAC columns with silica fume and hybrid fiber. J. Build. Struct. 34 (5), 122–129. https://doi.org/10.14006/j.jzjgxb.2013.05.014.

Wang, Y.G., Hughes, P., Niu, H.C., Fan, Y.H., 2019. A new method to improve the properties of recycled aggregate concrete: composite addition of basalt fiber and nano-silica. J. Clean. Prod. 236, 117602 https://doi.org/10.1016/j.jclepro.2019.07.077.

Wei, T., Quan, X.Y., Yan, Q.Q., Wang, C.X., 2019. Experimental study on mechanical properties of recycled concrete with high ductility iron tailings. Concr. Cem. Prod. 8, 93–96. https://doi.org/10.19761/j.1000-4637.2019.08.093.04.

Xiao, B., An, X.W., Yang, R., Han, Y.Z., Huang, T.X., Guo, Z.Q., 2018. Experimental research on basic mechanical characteristics of recycled aggregate concrete and influencing factors. Concrete 11, 32–36. https://doi.org/10.3969/j.issn.1002-3550.2018.11.009.

Xu, Y.Z., 2019. Preparation and Mechanical Properties of High Volume Iron Tailings Sand Concrete. Shenyang University of Technology, Shenyang.

Xu, S.H., Li, A.B., Cui, H.P., Liu, X.W., 2016. Experimental investigation of the stress-strain relationship of carbonated concrete under monotonic loading. Build. Struct. 46 (6), 81–85. https://doi.org/10.19701/j.jzjg.2016.06.014.

Xu, W.T., Wen, X.L., Wei, J.X., Xu, P., Zhang, B., Yu, Q.J., Ma, H.Y., 2018. Feasibility of kaolin tailing sand to be as an environmentally friendly alternative to river sand in construction applications. J. Clean. Prod. 205, 1114–1126. https://doi.org/10.1016/j.jclepro.2018.09.119.

Yang, T., Wang, S.L., Liu, W., 2017. Restoring-force model of modified RAC columns with silica fume and hybrid fiber. J. Cent. South. Univ. 24 (11), 2674–2684. https://doi.org/10.1007/s11771-017-3680-9.

Yuan, C.F., Niu, D.T., Chen, N., Duan, F.Z., 2013. Influence of carbonation on the microstructure of concrete. Bull. Chin. Ceram. Soc. 32 (4), 687–707. https://doi.org/10.16552/j.cnki.issn1001-1625.2013.04.011.

Zhang, B.Z., Wang, S.L., Zhang, B., Jing, L.P., Shi, C.Y., 2011. Experimental analysis of the basic mechanical properties of recycled concrete. Concrete 7, 4–6. https://doi.org/10.3969/j.issn.1002-3550.2011.07.002.

Zhang, G.D., Zhang, X.Z., Zhou, Z.H., Cheng, X., 2013a. Preparation and properties of concrete containing iron tailings/manufactured sand as fine aggregate. Adv. Mater. Res. 838–841, 152 - 155. https://doi.org/10.4028/www.scientific.net/AMR.838-841.152.

Zhang, X.Y., Song, Q., Li, H., Fan, X.D., 2013b. Effect of iron tailings powder on properties of C40 concrete. Bull. Chin. Ceram. Soc. 32 (12), 2559–2563. https://doi.org/10.16552/j.cnki.issn1001-1625.2013.12.022.

Zhang, L.F., Han, J.D., Liu, W.Q., Sun, W., 2015. Microstructure evolution of cement-based materials caused by carbonation reaction-A review [J]. Mater. Rep. A: Rev. 29 (2), 85–95. https://doi.org/10.11896/j.issn.1005-023X.2015.03.016.